

Fatigue Behavior of Welded Joints Part 2: Physical Modeling of the Fatigue Process

Two complementary models were developed to predict fatigue behavior of joints in fillet welds

BY P. DARCIS, T. LASSEN, AND N. RECHO

ABSTRACT. The fatigue process in fillet welded joints is discussed and modeled. As a first approximation, a pure fracture mechanics model was employed to describe the entire fatigue process. The model is calibrated to fit the crack growth measurements obtained from extensive testing on fillet weld joints where cracks emanate from the weld toes. Emphasis is laid on the choice of growth parameters in conjunction with a fictitious initial crack size distribution in order to obtain both reliable crack growth histories and predictions of the entire fatigue life. The model has its shortcomings in describing the damage evolution at low stress ranges due to the presence of a significant crack initiation period in this stress regime. As an alternative to the fracture mechanics model, a two-phase model (TPM) for the fatigue process was developed and calibrated. The number of cycles to crack initiation was modeled by a local strain approach using the Coffin-Manson equation, whereas the propagation phase was modeled by fracture mechanics, adopting the simple version of the Paris law. The notch effect of the weld toe was treated by extreme value statistics for the weld toe radius. To make the model fit all test data for crack initiation and propagation, it is crucial to select a sufficiently low transition depth between the two phases. A transition depth of 0.1 mm (0.004 in.) was selected. Furthermore, the material parameters in the Coffin-Manson equation were determined directly from the early cracking in the weld toe for full-scale fillet welds and not from tests carried out with small-scale smooth specimens. This is essential if the model is to account for the actual surface condition at the weld toe. The S-N curves constructed by the present physical model were compared with the

median nonlinear S-N curve obtained from the statistical random fatigue-limit model (RFLM) presented in Part 1 of this investigation. The curves are almost identical in the stress region where experimental data exist and both models fit the experimental data very well. However, the TPM does not predict any fatigue limit, in contrast to the RFLM. According to the TPM, the long fatigue life found at low stress ranges is a result of a dominating long initiation period and is not a threshold phenomenon. The two models are complementary tools. The RFLM is a pure statistical model, whereas the TPM is a semiempirical physical model. The TPM is capable of taking into account the effect of the global geometry of the joint, the local weld toe geometry, applied stress ratio, and the residual stress condition. Both models can be used for fatigue life predictions, but only the physical TPM can be used for planning of in-service inspection strategies where damage evolution as a function of time is needed.

Introduction and Objectives

In this investigation, the fatigue process in fillet-welded joints where cracks emanate from the weld toe was studied and modeled. In Part 1, a statistical model based on a joint random fatigue life and a random fatigue limit [random fatigue-limit model (RFLM)] was applied to predict the fatigue life of these types of joints. The S-N curve obtained from this

RFLM was nonlinear for a log-log scale between the stress range ΔS and number of cycles N to failure. The model fits the assembled S-N data in the low stress region far better than the traditional bilinear S-N curve found in rules and regulations. The fatigue behavior is obviously significantly more complex at low stress ranges than the conventional curves are able to describe. The RFLM-based nonlinear curves give some new physical insight into the fatigue process itself and this is pursued in this investigation by a semiempirical physical model. The model is a complementary tool to the statistical RFLM developed in Part 1. It is important to control the physical parameters that have an influence on the fatigue damage process as it evolves toward final failure. This is important when the following predictions are required:

- Predictions of fatigue life under conditions for which experimental data do not exist
- Predictions of likely crack growth histories leading to failure.

The need for a more physical model for carrying out the first type of predictions is obvious; fatigue life can only be predicted by a statistical model for joints pertaining to the populations and conditions for which the model was established. If basic fatigue properties such as joint geometry or loading modes are changed, it is only a physical model that can predict the effect of such changes on the fatigue life. Hence, the physical model is an important tool in safe life analysis. The second type of predictions are required if inspection planning is to be carried out, i.e., a damage tolerance approach. In this case it is a necessity to characterize the fatigue process itself, not only to determine the final fatigue life. This is essential if in-service inspections are to be planned; we must know what crack sizes to look for at different times before final failure. This will make the scheduled inspection more efficient and economical. Based on these considerations, a physical model will be

KEYWORDS

Welded Steel Joints
Fatigue Behavior
Influencing Physical Parameters
Crack Initiation
Crack Propagation
Life Predictions
Constructed S-N Curves

P. DARCIS and N. RECHO are with LERMES, Laboratoire d'Etudes et de Recherche en MEcanique de Structures, Université Blaise Pascal, Clermont II, France. T. LASSEN is with Agder University College, Faculty of Engineering, Grimstad, Norway.

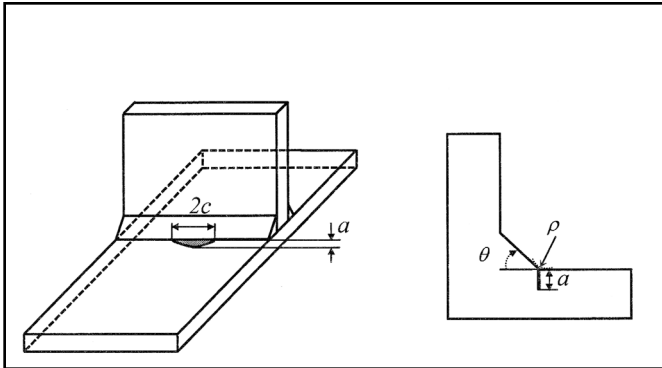


Fig. 1 — Joint configuration with crack shape parameters a and c .

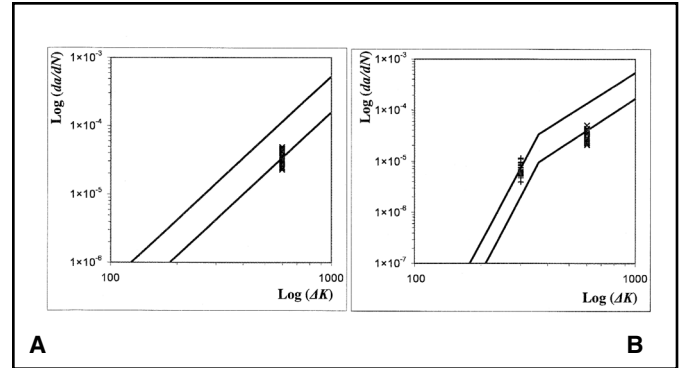


Fig. 2 — Growth parameters obtained from experiments together with the BS 7910 scatter-band. A — Linear relationship; B — bilinear relationship.

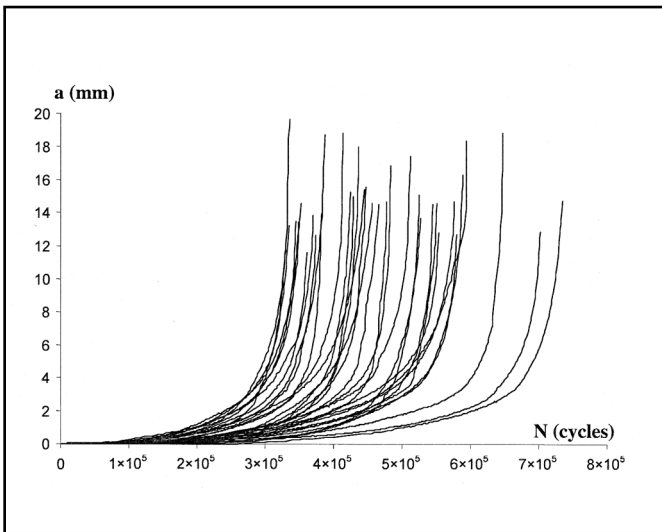


Fig. 3 — Experimental a - N curve (Database 1).

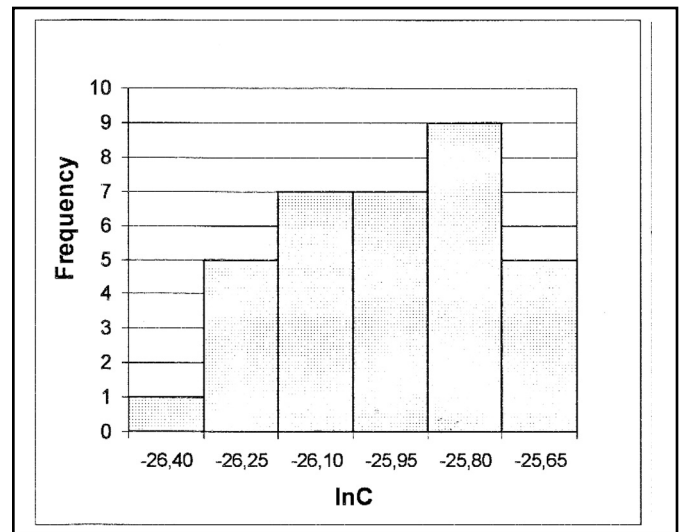


Fig. 4 — Histogram for $\ln C$ (MPa, m).

established to meet the following criteria:

- The model should be corroborated by S-N data for the joint in question when these are available. (Database 1 and 2 in Part 1.)
- The model should predict a crack evolution that coincides with measured crack growth histories before failure. (Database 1 in Part 1.)

With this background, we endeavored to model the fatigue process in fillet weld joints. The total fatigue life was considered to be the sum of the cycles spent in the crack initiation phase and the crack propagation phase:

$$N_T = N_i + N_p \quad (1)$$

For some time there has been a debate among researchers and engineers as to whether or not the crack initiation period is important. The traditional belief has been that fatigue crack growth often starts from surface-breaking defects in the weld toe region. The initial flaw has often been

assumed to have a depth greater than 0.1 mm, sometimes 0.25 mm. In rules and regulations, an initial crack depth even as deep as 0.5 mm (0.02 in.) has been recommended (Ref. 1). These flaws act as direct starters for the fatigue crack propagation and the fatigue initiation period can be neglected. However, with advanced fatigue testing where the entire crack depth history, and not only the final fatigue life, is monitored, it has become obvious that this simple approach does not fit the facts. Several researchers have obtained experimental evidence that supports the existence of a crack initiation period (Refs. 2, 3). The conclusion is that rather than speaking of small microcracks or inclusions in the vicinity of the weld toe, it is more correct to use the notion of unfavorable surface condition, which gives a rather short initiation period under accelerated laboratory conditions. The early damage mechanism is a combination of crack nucleation and microcrack growth. In welded joints subjected to high stresses

in accelerated laboratory conditions (typically stress range of 120–150 MPa (17.4–21.7 ksi)), the initiation period, defined as time to reach a crack depth of 0.1 mm, is typically 30% of the entire fatigue life (Ref. 3). This means that if the same joint is subjected to stress levels that are typical of service conditions (equivalent stress range 50–80 MPa (7.3–11.6 ksi)), the crack initiation will totally dominate the fatigue life. Due to this fact, a fracture mechanics model (FMM) will not be able to meet both of the model criteria listed above. With this background, a TPM was investigated and compared with the FMM as well as with the results obtained by the RFLM in Part 1 of this article. It was Lawrence et al. who first suggested the TPM and a good overview is given in Refs. 4 and 5. As the method now stands, its accuracy depends greatly on the calibration experiments. Our objective here is to elaborate and calibrate the model to fit the various test series that were presented in Part 1. The predictions made by the model

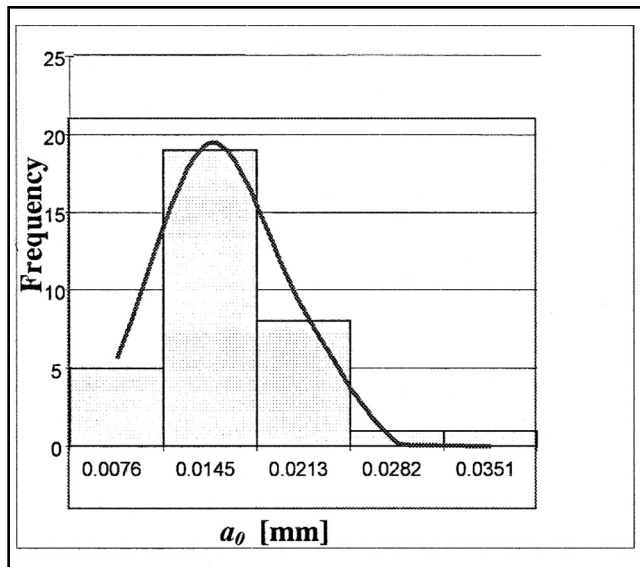


Fig. 5 — Histogram for the initial crack depth.

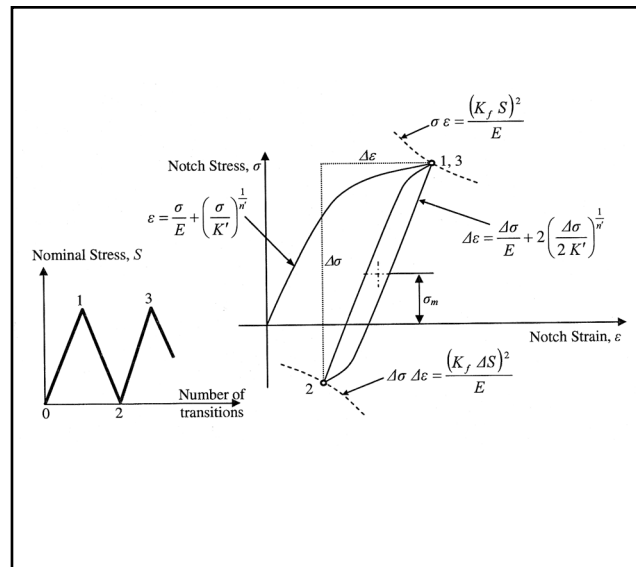


Fig. 6 — Schematic illustration of the local stress-strain hysteresis loop analysis.

Table 1 — Statistics for Local Weld Toe Geometry, Database 1

Weld toe angle θ (degrees)		Weld toe radius ρ (mm)	
Mean	Standard Deviation	Mean	Standard Deviation
58	9	1.6	0.7

Table 2 — Measured Number of Cycles (in 1000) Spent in Various Phases, Accelerated Laboratory Condition 150 MPa (Database 2)

N_i is defined as time to reach 0.1 mm			
N_i	N_p	N_f	N_f , F-class
140	330	468	513

will be compared with the predictions made by the RFLM in Part 1.

The Fracture Mechanics Approximation

Before developing the TPM we shall present a brief overview of the fracture mechanics model and point out its shortcomings when it comes to describing the entire fatigue process for high-quality welds. It is assumed that the FMM can predict the propagation rate of a semi-elliptical crack, as shown in Fig. 1, from its initial crack depth to final critical crack depth. By integration of the Paris law the number of cycles to failure can be presented in an S-N format:

$$N = \frac{1}{C} \int_{a_0}^{a_c} \frac{da}{(\Delta S \sqrt{\pi a} F(a))^m} \quad (2)$$

where C and m are treated as material parameters for a given mean stress and environmental condition. $F(a)$ is a dimensionless geometry function accounting for loading mode, crack, and joint geometry. The equation is valid when the stress intensity factor range (SIFR) $\Delta K = \Delta S \sqrt{\pi a} F(a)$ is greater than the threshold

value ΔK_0 . Below this threshold value, it is assumed that the crack will not grow. Recommendations are given in BS 7910 (Ref. 6) for the growth rate parameters C and m and the threshold value ΔK_0 . The geometry function $F(a)$ is also given. Regarding the parameters C and m , two alternatives are suggested for the relationship between the growth rate da/dN and the SIFR for a log-log scale. The first alternative is based on a single linear relationship, whereas the second alternative proposes a bilinear relationship — Fig. 2. The data points on the figure are derived from growth measurements and are discussed below. The main difference between the two models is that the bilinear one models the gradual decrease in the growth rate for low values of the SIFR before the threshold value is finally reached. As a first approximation, the FMM was used to fit all the measured growth histories given in Fig. 3 (Database 1). Each of the 34 curves was fitted by the FMM by adopting the slope m given for the growth curves in Fig. 2. For each fit the parameters a_0 and C were determined. The a-N curves obtained from the FMM were quite close to the experimental ones in Fig. 3. This was true for both the single linear and bilinear relationships between the growth rate and the SIFR. Details from this analysis are found in Ref. 7. A histogram for the natural logarithm of C derived under the assumption of a single

linear relationship between the crack growth rate and the SIFR for a log-log scale is shown in Fig. 4. In rules and regulations, the distribution of $\ln(C)$ is assumed to be normally distributed (as the fatigue life is assumed lognormally distributed). The present distribution is not obviously a normal distribution. The results are also plotted in Fig. 2 and compared with BS 7910 recommendations. As can be seen, the results are in good agreement with the mean line given in BS 7910. This was not the case for the results derived for the bilinear relationship. The growth rates are close to four times higher than the mean values given in BS 7910 for the lower line segment — Fig. 2. These high growth rates are probably due to the fact that the lower part of the bilinear curve is derived from tests with relatively long cracks (several millimeters) in compact tension specimens. The fatigue process in welded joints comprises crack growth of small surface-breaking elliptical cracks with depths less than 0.1 mm. These cracks may grow considerably faster than the lower part of the bilinear growth curve in BS 7910 prescribes. Hence, one should take care when using the bilinear relationship given in BS 7910 to calculate the early fatigue crack growth in welded joints.

The statistics for the calculated initial

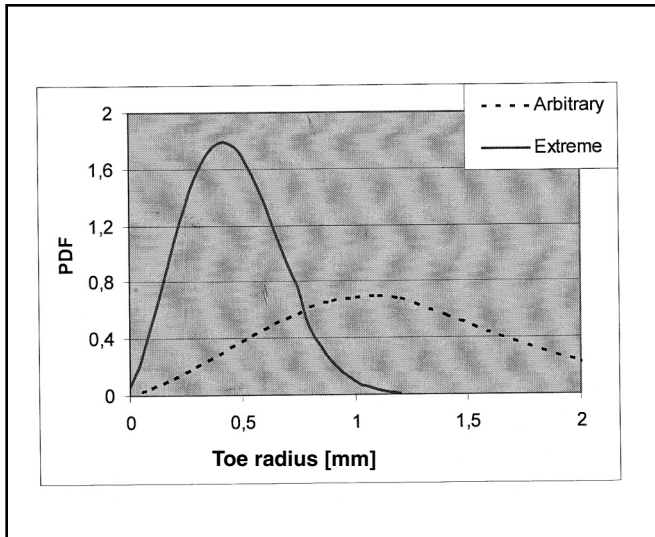


Fig. 7 — Definition of the toe notch geometry in one specimen by extreme value statistics.

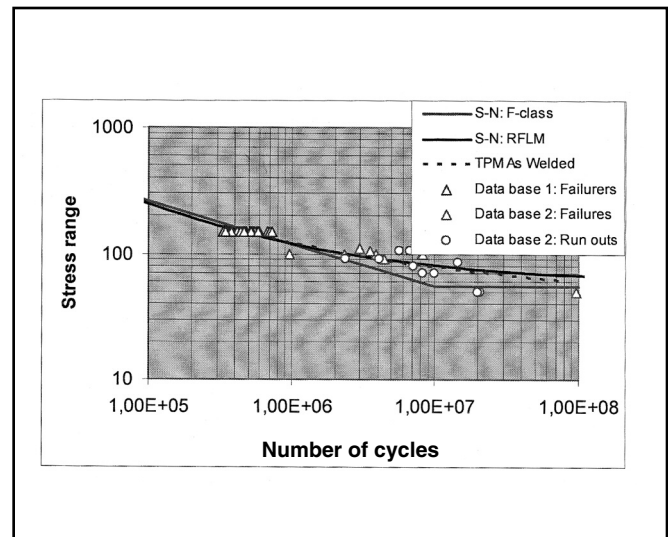


Fig. 8 — S-N curves constructed from the RFLM and TPM together with the F-class median curve and test data.

Table 3 — Cyclic Mechanical Properties and Parameters in the Coffin Manson Equation Calibrated for Time to Reach 0.1 mm, HB = 202

Parameter, Symbol (units)	Value
Cyclic yield stress, S'_y (MPa)	424 (61 ksi)
Ultimate strength, S'_u (MPa)	697 (101 ksi)
Young modulus, E (GPa)	206 (30000 ksi)
Fatigue strength exponent, b	-0.089
Fatigue strength coefficient, σ'_f (MPa)	1032 (150 ksi)
Fatigue ductility exponent c	-0.6
Fatigue ductility coefficient ϵ'_f	0.81
Cyclic strength coefficient, K' (MPa)	1064 (154 ksi)
Strain hardening exponent, n'	0.148

crack depths a_0 are given in Fig. 5. The mean value is 0.015 mm (0.0006 in.) and the upper bound is close to 0.03 mm (0.0012 in.). It should be emphasized that this initial crack depth distribution is a purely theoretical concept, i.e., it cannot be proven that the crack depths are related to initial flaws created by the welding process. The derived mean values for the a_0 , C , and m are substituted into Equation 2 to calculate both crack evolution and fatigue life at various constant amplitude stress levels. Both the linear and bilinear relationship is used. The following shortcomings were revealed: the predictions made by the linear relationship correspond to the predictions made by the S-N curve F-class above the fatigue limit, whereas the predictions made by the bilinear curve do not. It is also to be noted that both the F-class and the FMM fail to predict the long experimental lives given by the data points in Database 2 at low stress levels. In addition, the FMM fails to predict the fatigue limit. Based on the fracture mechanics threshold criterion,

$\Delta S_0 = \sqrt{\pi a_0} F(a_0) = \Delta K_0$, the fatigue-limit is 95 MPa based on the initial cracks given in Fig. 5. This is far too high compared with the limit of 56 MPa given by the F-class and 60 MPa obtained from the RFLM. The reason is the same as for the discrepancy found between the experimental growth rates and the growth rates given in the lower part of the bilinear relationship in BS 7910. Both the prescribed drop in the growth rate and the final stop at low SIFR are valid for larger cracks only. They are not applicable to shallow elliptical cracks at the weld toe. In conclusion, the FMM should not be used to model the entire fatigue process in high-quality welds proven free from detectable initial cracks. Although the model is capable of describing the crack evolution at one given stress level, it will fail to predict the change in slope of the S-N curve as the stress range decreases. Furthermore, the fatigue-limit will be overly optimistic. The FMM should only be applied if cracks are found and sized. In other cases a crack initiation phase should be modeled before

the crack propagation phase is added on. This is shown in the next section.

Modeling the Fatigue Crack Initiation Period

Basic Concept and Equations for the Local Stress-Strain Approach

The predictions for the number of cycles to crack initiation, N_i , are based on the Coffin-Manson equation with Morrow's mean stress correction (Refs. 4, 5):

$$\frac{\Delta \epsilon}{2} = \frac{(\sigma'_f - \sigma_m)}{E} (2N_i)^b + \epsilon'_f (2N_i)^c \quad (3)$$

Here $\Delta \epsilon$ is the local strain range and σ_m is the local mean stress at the weld toe. The parameters b and c are the fatigue strength and ductility exponents, and σ'_f and ϵ'_f are the fatigue strength and ductility coefficients, respectively. The local stress and strain behavior is given by the Ramberg-Osgood stabilized cyclic strain curve:

$$\Delta \epsilon = \frac{\Delta \sigma}{E} + 2 \left(\frac{\Delta \sigma}{2K'} \right)^{1/n'} \quad (4)$$

where K' and n' are the cyclic strength coefficient and strain hardening exponent, respectively. Equation 4 is combined with the Neuber rule as follows:

$$\Delta \epsilon \Delta \sigma = \frac{(K_t \Delta S)^2}{E} \quad (5)$$

where ΔS is the nominal stress range, E is

Young's modulus, and K_t is the stress concentration factor at the welded toe. Equation 5 is sometimes modified by introducing the fatigue notch factor K_f instead of K_t . It is argued that the fatigue notch factor better quantifies the severity of a discontinuity in the fatigue life calculation. Yung and Lawrence concluded (Ref. 4) that Peterson's equation correctly interrelates the fatigue notch factor to elastic stress concentration factors for welded joints:

$$K_f = 1 + \frac{(K_t - 1)}{1 + \left(\frac{a_p}{\rho}\right)} \quad (6)$$

Here ρ is the weld toe root radius and a_p is Peterson's material parameter. The latter may be approximated by the expression $1.087 \times 10^5 S_u^{-2}$ (in mm, N/mm²) where S_u is the tensile strength of the steel. The following expression for K_t is used (Ref. 8):

$$K_t = 1 + \left[0.5121(\theta)^{0.572} \left(\frac{T}{\rho}\right)^{0.469} \right] \quad (7)$$

where θ is the weld toe angle (radians) and T is the plate thickness — Fig. 1.

The definition of the local stress-strain variation is illustrated in Fig. 6. The nominal stress S (left) and the local stress σ (right) are shown for the first reversal (0-1) and the stabilized hysteresis loop (1-2-3). The local $\Delta\sigma$ and $\Delta\varepsilon$ and the mean stress, σ_m , corresponding to the cyclic loading, are determined. The effect of cyclic hardening or cyclic softening is neglected.

In the case of an elastic notch root condition at the weld toe, Equation 3 reduces to the Basquin equation, neglecting the second term on the right-hand side. This equation can be rearranged as follows:

$$N_i = \frac{1}{2} \left(\frac{K_f \Delta S}{2(\sigma'_f - \sigma_m)} \right)^{1/b} = \frac{1}{2} \left[\frac{2(\sigma'_f - \sigma_m)}{(K_f \Delta S)} \right]^{-1/b} \quad (8)$$

From this equation one may construct an S-N curve with slope b .

Definition of the Initiation Phase and Determination of Parameters

When applying the Coffin-Manson approach to predict time to crack initiation

at the weld toe, three questions arise. The first is what stress concentration factor K_t one should choose to characterize the notch effect from the highly variable local toe geometry. The next is the definition of time to crack initiation, i.e., what crack depth is reached at the end of the phase before propagation is considered to take over. This depth will be referred to as the transition depth. If too large a depth is chosen, the initiation phase will not obey Equation 3 due to the substantial amount of crack

growth involved. Several definitions are possible for the transition depth and this is probably one of the reasons why so few two-phase models have been applied in practice. The last question is how to determine the cyclic mechanical parameters and the parameters in the Coffin-Manson equation such that they are valid for the weld toe condition. Usually these parameters are determined from tests with small-scale smooth specimens. However, in a full-scale weld there may be size effects and surely surface finish effects involved. Tests with smooth specimens may not be representative for the rough surface conditions found in the vicinity of the weld toe. It is our hypothesis that the actual parameters should be determined directly from full-scale tests with welded joints where the early cracking is measured. Database 1 gives us this possibility. Based on the discussion above we will emphasize three topics:

- Local toe geometry and stress concentration factor
- The choice of the transition depth
- The determination of the parameters in Coffin-Manson law.

Local Toe Geometry and Stress Concentration Factor

The statistics for the local geometry for the specimens tested in series 1 (Database 1) are given in Table 1. If we substitute the mean values in Table 1 into Equation 7 this will give $K_t = 2.9$. This value is corroborated by a refined finite element analysis. However, it is highly likely that the cracks initiate at a more unfavorable geometry. It is above all the variability in the toe radius

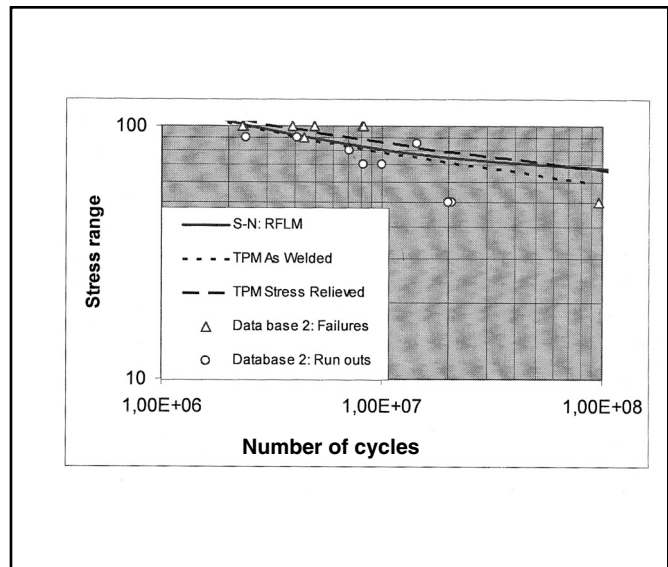


Fig. 9 — S-N curves constructed from the RFLM and TPM in the low-stress region.

that yields K_t values in the range from 2.9 to 7. To circumvent this problem of variability, Lawrence et al. suggested using the fatigue notch factor K_f instead of K_t . Furthermore, a worst-case notch was defined by setting the toe radius equal to the Peterson constant in Equation 6. In our case this will approximately give $\rho = a_p = 0.3$ mm, which corresponds to $K_f = 3.1$. The problem with the K_f concept is that the physical interpretation is not obvious. It has been claimed (Ref. 9) that the need for a definition of a fatigue notch factor is due to the fact that the crack initiation life in reality includes an appreciable amount of crack growth. If the initiation phase were limited to pure nucleation of a microcrack, the stress concentration factor could have been used directly in the calculations. Furthermore, the smallest radius in a joint is a random variable and its mean value will be a function of the length of the welded joint. This is pursued below. Let us set the toe angle constant at the mean value and try to determine the most likely smallest toe radius found within one test specimen. The statistics in Table 1 were derived from 300 measurements taken with 5.5-mm spacing along a welded joint with a total length 1650 mm. It appeared that two neighboring radii with a spacing of 5.5 mm could be very different, whereas at a closer distance there is a correlation. Based on this observation we assume that at a 5.5-mm spacing the measured radii will be independent. Hence, a welded joint with length W mm contains $k = W/5.5$ totally independent radii. The extremum distribution for the smallest value will then read:

$$1 - F_{\rho_{min}}(\rho) = (1 - F_{\rho}(\rho))^k \quad (9)$$

where $F_p(\rho)$ is the cumulative distribution function (CDF) of an arbitrary radius as given in Table 1, whereas $F_{pmin}(\rho)$ is the CDF for the smallest value over the length W . The mean and peak values for this smallest radius can be derived from the corresponding probability density function (PDF). The peak value is by definition the most likely value for the smallest radius within the length W . If we assume that ρ is Weibull distributed (Ref. 10) and W is set to 1650 mm ($k = 300$), then our approach will give a peak value for the smallest radius close to 0.1 mm. The smallest radii found in various test series are actually close to 0.1 mm (Ref. 10). Hence, these results support our approach. If we use the same approach within the width of one test specimen ($W = 60$ mm, $k = 60/5.5 = 10$), we get $\rho = 0.42$ mm. The PDFs are shown in Fig. 7. As can be seen, the mean value and the peak value are not very different for the relatively narrow symmetrical extreme value distribution. The resulting figures will give a stress concentration factor of 4.5 that will be used in our calculations.

Transition Depth

In earlier work, the transition depth has often arbitrarily been set to 0.25 mm (0.01 in.). However, the time to develop such a deep crack will include a large amount of crack growth. This has in many cases resulted in models that give reasonably good predictions at short fatigue lives (less than 10^6 cycles), but an overprediction of the fatigue lives for low stress levels. The reason is that the initiation part at low stress levels will have a life curve with a slope close to the parameter $b \cong -1/10$ (see Equation 8). This is only true for pure initiation, whereas crack growth will have a slope according to the Paris law, $1/m \cong -1/3$ relative to the applied stress range. Hence, a phase that contains both nucleation and growth will have a slope between $-1/3$ and $-1/10$. If a slope of $-1/10$ is assumed for such a mixed process, it will overestimate the fatigue life significantly at low stresses. In more recent work, Lawrence et al. (Ref. 5) suggested that the transition depth should be between 0.05 and 0.1 mm. In the present work, we investigated the results obtained by setting the transition depth equal to the lower and upper bound of this given range. The following arguments support a transition depth of 0.1 mm (0.004 in.):

- To apply the fracture mechanics model at crack depths smaller than 0.1 mm may be dubious because one approaches the grain size of the steel (typically 0.01 mm).
- In laboratory tests it is hardly possible to measure any crack less than 0.1 mm with

sufficient accuracy without using destructive methods.

- Cracks with a depth below 0.1 mm are not of interest in in-service inspection as no common nondestructive examination method can detect such small cracks. Hence, for inspection planning we do not need the notion of a crack smaller than 0.1 mm.

Our arguments are partly theoretical, partly practical. The actual number of cycles to reach 0.1 mm is given in Table 2 for Database 1. In contrast to the fictitious initial crack depths obtained from the FMM analysis in the previous section, this is a measurable quantity. The fatigue initiation life is close to 30% of the entire fatigue life. The entire fatigue life is 10% shorter than the predictions from the F-class curve. The arguments for a transition depth of 0.05 mm are less obvious. It is to be noted that even this shallow depth is well above the initial crack distribution obtained from the fracture mechanics model (see Fig. 5). The upper bound was found to be 0.03 mm for these cracks. Hence, the transition depth of 0.05 mm is about the smallest transition depth possible based on what may be interpreted as crack size of possible initial flaws. The time to arrive at 0.05-mm crack depth was not measurable for the tests carried out for Database 1. The number of cycles to reach this depth can be found by backcalculation from the first measurable crack size (0.1 mm) by applying the fracture mechanics model. In this way the number of cycles to reach 0.05 mm was determined to 90,000 cycles, i.e., 20% of total fatigue life.

Cyclic Mechanical Properties and Parameters in Coffin-Manson Equation

It is our hypothesis that parameters determined from small-scale smooth specimens are not directly applicable for weld toe conditions. Hence, we will determine these parameters directly from the time to early cracking as given Table 2. We now seek the parameters in Equations 3 and 4 that correspond to the initiation time given in Table 2. The calibration is carried out by assuming a dependency between the various parameters with the Brinell hardness (HB) as the key parameter. The following equations were applied (Ref. 11):

$$\begin{aligned}
 S_u &= 3.45 \text{ HB} & \text{MPa} & & n' &= \frac{b}{c} \\
 S_y &= 0.608 S_u & \text{MPa} & & K' &= S_y (0.002)^{-n'} \text{ MPa} \\
 b &= -0.1667 \log \left(2.1 + \frac{917}{S_u} \right) & & & \sigma_f' &= 0.95 S_u + 370 \text{ MPa} \quad (10) \\
 c &= -0.7 < c < -0.5 & & & \epsilon_f' &= \left(\frac{\sigma_f'}{K'} \right)^{1/n'}
 \end{aligned}$$

where S_u and S_y are the tensile stress and yield stress respectively, and S_y is the

cyclic yield stress. The correlation between the various parameters, using the HB as a master variable, is not exact. In Ref. 12, it was found that the relationship might lead to significant overestimation of the initiation life. Furthermore, Dowling (Ref. 9) suggested that the surface condition at the weld toe would primarily alter the fatigue strength exponent b . However, in the present work we accept the relationships given in Equation 10 but not the absolute values. An absolute value is sought such that the time to reach a given transition crack depth coincides with what actually has been measured on the welded joints in Database 1. The solution gives a HB close to 202 for the cycles to reach a crack depth of 0.1 mm. This HB is very close to the value actually measured in the HAZ of the weld toe. The values measured for the base metal was HB = 145 and value of the HAZ was 213. Hence, our solution is only 5% less than the highest value measured at the potential crack locus. If we had applied HB = 213 directly, the solution would give the time to reach a crack depth of 0.3 mm. Hence, a significant amount of crack propagation would have been included in the initiation phase. When using the search scheme for determining the parameters with a transition depth of 0.05 mm, we obtained a HB of 180, i.e., still within the range measured on the specimens, but 15% less than the value at the HAZ.

The parameters corresponding to HB = 180 ($a = 0.05$ mm) and HB = 202 ($a = 0.1$ mm) were used in Equations 3 and 4 to define the first part of the TPM. The propagation phase (Equation 2) was subsequently added to calculate the entire fatigue life. The model predicts exactly the mean value for the fatigue lives of Database 1 at a stress range of 150 MPa (21.7 ksi). When the stress range was decreased from 150 MPa (21.7 ksi) to below 100 MPa (14.5 ksi), the model based on a transition depth of 0.1 mm predicted somewhat longer lives than the median line obtained from the RFLM, which is representative for Database 2 in this stress region. The model based on a transition depth of 0.05 mm predicted results somewhat shorter lives than figures obtained from the RFLM in this region. At a stress range of 80 MPa, the model with $a = 0.1$ mm predicts 28% longer life than the median line of the RFLM, whereas the model with $a = 0.05$ mm predicts 20% shorter life than the same median line. These results are discussed more in detail in the next section. The results indicate that the interval for a transition depth between 0.05 and 0.1 mm as proposed by Lawrence et al. (Ref. 5) is a reasonable choice. Furthermore, any transition depth in this narrow band will predict fatigue life well within the scatter band of Database 2. Based on the ar-

guments given in the beginning of this section, we have selected a transition depth of 0.1 mm in what follows. The corresponding parameters in the Coffin-Manson equation are given in Table 3. As we already have shown, the solution given in Table 3 is not unique. Other solutions without total dependency between the parameters are possible. However, these solutions will not be far from the one given in Table 3. Hence, we regard the solution representative of prediction of time to reach a depth of 0.1 mm in welds made from C-Mn steel with a yield stress close to 345 MPa (50 ksi).

Constructing the S-N Curve from the Two-Phase Model

One of our main goals is to construct S-N curves from the TPM that are consistent with the RFLM curves obtained in Part 1 of this investigation. As pointed out in Part 1, the RFLM curve fits the data points far better than the F-class curve at low stress ranges. Although the TPM is semiempirical, it has a more physical-theoretical basis than the RFLM, which is based on purely statistical methods. The TPM is capable of predicting the influence of, for instance, local weld toe geometry, stress ratio, and stress relieving. Thus, high-quality joints will have long fatigue lives, whereas poor quality will be penalized. The TPM model can also be applied to calculate fatigue lives at low stress levels where experimental data do not exist and where it is dubious to extrapolate the statistical RFLM.

Let us begin by demonstrating that the model can predict fatigue lives that are in good agreement with the S-N curve obtained from the RFLM under appropriate assumptions of the quality of the joint. For joints that are stress relieved (Database 1), the TPM will predict fatigue lives as given in Table 4 at various stress levels. As can be seen from the table, the time to crack initiation at a test stress range of up to 150 MPa (21.7 ksi) is 30% of the entire fatigue life, whereas it is 88% of the fatigue life at a stress range of up to 80 MPa (11.5 ksi). These results pinpoint the importance of the crack initiation life at low stress ranges, i.e., in the stress region where service stresses usually occur. The table also lists the fatigue lives predicted by the RFLM and the F-class. At stress ranges below 100 MPa (14.5 ksi), the TPM predicts somewhat longer lives than the S-N curve based on the RFLM and significantly longer lives than the F-class S-N curve. As can be seen from Table 4, the total TPM fatigue life is close to 1.6 times longer than the life obtained from the RFLM and 5.5 times longer than prediction made by the F-class at 80 MPa (11.5 ksi).

When comparing these figures we must

Table 4 — Results Derived from the TPM at Various Stress Ranges. Stress Relieved (SR), R = 0.3

Stress Range (MPa)	N_i (cycles) TPM	N_p (cycles) TPM	N_i (Cycles) TPM	N_i/N_t % TPM	N_i RFLM	N_i F-class
150	1.4×10^5	3.3×10^5	4.7×10^5	30	4.6×10^5	5.1×10^5
120	5.6×10^5	6.5×10^5	1.2×10^6	47	1.1×10^6	1.0×10^6
100	2.1×10^6	1.1×10^6	3.2×10^6	66	2.5×10^6	1.7×10^6
80	1.6×10^7	2.2×10^6	1.8×10^7	88	11.0×10^6	3.4×10^6
60	3.7×10^8	5.1×10^6	2.9×10^8	99	∞	8.0×10^6

Table 5 — Results Derived from the TPM at Various Stress Ranges. As Welded (AW), R = 0.1

Stress Range (MPa)	N_i (cycles) TPM	N_p (cycles) TPM	N_i (cycles) TPM	N_i/N_t % TPM
150	1.3×10^5	3.3×10^5	4.6×10^5	28
120	4.3×10^5	6.4×10^5	1.1×10^6	40
100	1.3×10^6	1.1×10^6	2.4×10^6	54
80	6.6×10^6	2.2×10^6	8.8×10^6	75
60	8.1×10^7	5.1×10^6	8.5×10^7	94

bear in mind that the figures derived from the TPM correspond to the test series in Database 1, i.e., stress relieved (SR) and with an applied stress ratio of $R = 0.3$. This stress relieving has a strong bearing on the time-to-crack initiation through the Morrow mean stress effect at long lives (Equation 3). The RFLM S-N curve is dominated by Database 2 in the low stress region. These tests are carried out on non-load-carrying fillet weld joints with thicknesses in the range of 16 to 38 mm. The specimens are all in the as-welded (A-W) condition and with a positive stress ratio, i.e., there may be large residual stresses present in the specimens. Furthermore, the vast majority of tests used to determine the F-class curve are in A-W conditions and often tested at a stress ratio close to $R = 0.1$.

Thus, our next step is to simulate these conditions for the initiation part of the TPM by setting the residual stress equal to the actual material yield stress, i.e., 400 MPa (58 ksi). The results are given in Table 5. As can be seen, the TPM results are now almost identical to the nonlinear S-N curve obtained from the RFLM, but the model still predicts a fatigue life 2.5 times longer than the F-class at 80 MPa (11.5 ksi). These results are illustrated in Fig. 8 where the F-class and RFLM-based S-N curves are drawn together with the TPM S-N curve and the test results. As can be seen, we have basically two types of curves. The F-class curve is bilinear, whereas the RFLM and TPM curves are continuously changing slope. All three S-N curves coincide at high stress levels. Hardly any discrepancy in fatigue life (less than 10%) is found above a stress range level of 120 MPa (17.4 ksi). When the

stresses are lowered to under 100 MPa, the RFLM curve and the TPM curve still coincide, but they predict 2–9 times longer lives than the F-class curve as long as the stress range is above the F-class fatigue-limit of 56 MPa (8.1 ksi). It is our judgment that the F-class curve is too conservative in the stress region under consideration, as was already discussed in Part 1. This is due to the fact that it is a straight line and based on test results that have the center of gravity for the stress ranges between 120 and 150 MPa (17.4 and 21.7 ksi). Hence, the curve fails to take into account the increasing fatigue life due to the importance of an initiation phase below 100 MPa. The experimental results plotted in this stress region corroborate the predictions made by the TPM. It has been shown how the TPM is capable of correctly taking into account the effect of residual stresses and loading ratio. This is shown in more detail in Fig. 9. The life curve obtained for the A-W condition coincides with the median curve (i.e., the RFLM curve) for Database 2.

Finally, it should be noted that although the statistically based RFLM and the physically based TPM give the same life predictions at almost any stress range level, there is one fundamental difference between them. The RFLM does prescribe a fatigue limit, whereas the TPM does not. This is illustrated in Fig. 9 where the focus is on the lower stress region. The slope of the S-N curve derived from the TPM will not be smaller than $b = -1/10$ and will never become horizontal as is the case with the RFLM. This gives a discrepancy between the curves at very long lives (longer than 10^8 cycles) such that the RFLM is more optimistic. The TPM pre-

dicts that any joint will eventually fail if the number of cycles is high enough. It is in fact possible to build a fatigue limit into the TPM by assuming that after crack initiation has taken place the crack may stop to grow, due to the fact that it has a SIFR below the threshold value. However, no data are available to corroborate such behavior for shallow surface-breaking cracks.

Conclusions

Our study was primarily carried out for non-load-carrying fillet weld joints made of C-Mn steel with nominal yield stress close to 345 MPa (50 ksi). A pure fracture mechanics model (FMM) and a two-phase model (TPM) were used to predict the fatigue life. The initiation life was modeled by the Coffin-Manson equation, whereas the crack propagation was based on the simple version of the Paris law. The models were validated and calibrated with the use of large databases. The criteria for acceptance of the models were that they should predict both damage evolution and final fatigue life at any stress level. The FMM failed to fulfill these criteria, whereas the TPM gave an excellent fit to both measured crack growth histories and experimental fatigue lives. The following conclusions were drawn.

The fatigue behavior of fillet weld joints is far more complex at typical in-service stresses than fracture mechanics can describe. This is due to the fact that the crack initiation phase dominates the fatigue life at these low stresses.

A TPM is capable of modeling the damage evolution from the initial state to the final fracture provided that the model is accurately calibrated for this purpose. The notch factor at the weld toe is based on extreme value statistics for the toe geometry, and the transition crack depth between the initiation phase and the propagation phase is set to 0.1 mm. The parameters in the Coffin-Manson equation were determined directly from early cracking in full-scale welded joints.

As the TPM has a semiempirical physical basis, the determining factors such as residual stresses, global and local joint geometry, and loading mode are readily accounted for.

The S-N curves constructed from the model are nonlinear for a log-log scale and coincide with the curves obtained from the statistical RFLM in Part 1 of this investigation. Both models fit experimental data far better than the conventional bilinear S-N curves.

There is a fundamental difference between S-N curves obtained from the RFLM and the TPM in the way that the latter curves do not predict any fatigue

limit. At stress ranges below 70 MPa the RFLM curve will appear flat, whereas the TPM curve will continue to fall with a small slope close to the parameter b in the Coffin-Manson law. At present there are no data to corroborate either one of these curves, but the authors tend to have more confidence in the prediction made by the physical-based TPM than the predictions based on the statistical RFLM when extrapolated outside the range of the data.

The first practical consequence of the present two-phase model is that it predicts longer lives at low stress ranges than the conventional S-N curves in rules and regulations. With the application of the TPM-constructed S-N curve in the lower stress region it is possible to reduce dimensions by 30–40% and still achieve the same fatigue life as for the F-class S-N curve.

The second practical consequence is that in-service inspection strategy may be optimized. This is due to the fact that the crack path leading to final fracture is quite different from the path calculated by a pure fracture mechanics model. The two-phase model with its long initiation phase will give a more hidden path for crack evolution. Hence, an inspection program with increased inspection frequency at the end of service life can be proven to be favorable.

Suggestions for Future Work

In this work, the TPM has been used to construct median S-N curves only. Future work should focus on constructing quantile curves for design purposes as well. This can be done by Monte Carlo simulation treating the main determining factors as random variables. The resulting curves should be compatible with the quantile curves obtained from the RFLM. Furthermore, as the TPM has no fatigue limit, it will be interesting to analyze how the model responds to variable loading by using a damage accumulation law. Finally, the practical consequences of the model in terms of joint dimensions and scheduled inspection programs should be studied in more detail. Other types of joints such as butt joints are also of great interest in this regard.

References

1. American Bureau of Shipping. 2003. *Guide for the Fatigue Assessment of Offshore Structures*. ABS, April.
2. Verreman, Y., and Nie, B. 1996. Early development of fatigue cracking at manual fillet welds. *Fatigue & Fracture of Engineering Materials and Structures* 19 (6): 669–681.
3. Lassen, T. 1990. The effect of the welding process on the fatigue crack growth in welded joints. *Welding Journal* 96(2): 75-s to 85-s.
4. Yung, J. Y., and Lawrence, F. V. 1985. Analytical and graphical aids for the fatigue design

of weldments. *Fatigue Fract. Engng. Mater. Struct.* 8: 223–241.

5. Lawrence, F. V., Dimitrakakis, S. D., and Munse, W. H. 1996. Factors influencing weldment fatigue. *Fatigue and Fracture, ASM Handbook*, Vol. 19, pp. 274–286. Materials Park, Ohio: ASM International.

6. BS 7910, *Guidance on Methods for Assessing the Acceptability of Flaws in Fusion Welded Structures*. 2000. London, U.K.: British Standards Institution (BSI).

7. Darcis, P. et al. 2004. A fracture mechanics approach for the crack growth in welded joints with reference to BS 7910. *European Conference on Fracture (ECF 15)*, Stockholm, Sweden, August 11–13, 2005.

8. Niu, X., and Glinka, G. 1987. The weld profile effect on the stress intensity factors in weldments. *Int. J. of Fracture* 35: 3–20.

9. Dowling, E. 1996. Estimating fatigue life. *Fatigue and Fracture, ASM Handbook*, Vol. 19, pp. 250–262. Materials Park, Ohio: ASM International.

10. Engesvik, K., and Lassen, T. 1988. The effect of weld toe geometry on fatigue life. *The 7th OMAE Conference*, Houston, Tex., pp. 441–445.

11. Testin, R. A., Yung, J. Y., Lawrence, F. V., and Rice, R. C. 1987. Predicting the fatigue resistance of steel weldments. *Welding Journal* 66: 93-s to 98-s.

12. Tricoteaux, A., Fardoun, F., Degallaix, S., and Sauvage, F. 1995. Fatigue crack initiation life prediction in high strength structural steel welded joints. *Fatigue Fract. Engng. Mater. Struct.* 18(2): 189–200.

REPRINTS REPRINTS

To order custom reprints
of articles in the
Welding Journal,
call FosteReprints at
(219) 879-8366 or
(800) 382-0808.

Request for quotes can be
faxed to (219) 874-2849.

You can e-mail
FosteReprints at
sales@fostereprints.com